C. R. Acad. Sci. Paris, Ser. I 357 (2019) 863–877

Contents lists available at ScienceDirect

C. R. Acad. Sci. Paris, Ser. I

www.sciencedirect.com

Partial differential equations/Dynamical systems

Turing patterns induced by cross-diffusion in a 2D domain with strong Allee effect

Motifs de Turing induits par réaction–diffusion croisée dans un système bidimensionnel avec un effet Allee fort

Naveed Iqbal [a], Ranchao Wu [b]

[a] *Mathematics Department, Faculty of Science, University of Ha'il, Ha'il 81451, Saudi Arabia*
[b] *School of Mathematical Sciences, Anhui University, Hefei, Anhui, 230601, PR China*

ARTICLE INFO

Article history:
Received 14 January 2019
Accepted after revision 23 October 2019
Available online 20 November 2019

Presented by the Editorial Board

ABSTRACT

In this work, we introduce a two-dimensional domain predator-prey model with strong Allee effect and investigate the Turing instability and the phenomena of the emergence of patterns. The occurrence of the Turing instability is ensured by the conditions that are procured by using the stability analysis of local equilibrium points. The amplitude equations (for supercritical case cubic Stuart–Landau equation and for subcritical quintic Stuart–Landau equation) are derived appropriate for each case by using the method of multiple time scale and show that the system supports patterns like squares, stripes, mixed-mode patterns, spots and hexagonal patterns. We obtain the asymptotic solutions to the model close to the onset instability based on the amplitude equations. Finally, numerically simulations tell how cross-diffusion plays an important role in the emergence of patterns.

RÉSUMÉ

Dans cette Note, nous introduisons un modèle prédateur–proie dans un domaine de dimension deux, avec effet Allee fort. Nous étudions l'instabilité de Turing et le phénomène d'émergence de motifs. L'apparition de l'instabilité de Turing est garantie par les conditions fournies par l'analyse de la stabilité des points d'équilibre locaux. Les équations d'amplitude (une équation de Stuart–Landau cubique dans le cas supercritique et quintique dans le cas sous-critique) sont établies en utilisant la méthode des échelles de temps multiples. On montre que le système admet des motifs comme des carrés, des bandes, des motifs en mode mixte, des taches et des motifs hexagonaux. Nous obtenons les solutions asymptotiques du modèle près de l'instabilité, à partir des équations d'amplitude.

E-mail address: naveediqbal1989@yahoo.com (N. Iqbal).

https://doi.org/10.1016/j.crma.2019.10.011
1631-073X/

Finalement, les simulations numériques montrent comment la diffusion croisée joue un rôle important dans l'apparition de motifs.

1. Introduction

Pattern formation has drawn considerable attention from the researchers in the past few decades because of its prime importance in the understanding of natural phenomena. In his seminal work, Turing [31] conveyed the idea of studying pattern formation with the help of reaction–diffusion systems. Reaction–diffusion models are well-known theoretical models that explain the self-regulated pattern formation in various areas of biology, chemistry, physics, ecology, geology, and in many other fields [6,8,31]. In the field of biology and ecology, the interaction among species and their evolution are significant behaviors [14,22,23,25,27,28]. The mathematical model is the key tool to investigate the interaction of species and their evolution, so various kinds of models have been studied in the past [3,4,10,11,15,17,18]. According to the ecological and biological point of view, the well-studied classic model of interaction among species is the predator-prey model.

According to the theoretical and experimental point of point, cross-diffusion plays an important role in the formation of patterns and has been extensively studied [1,32]. The phenomenon of the formation of patterns is commonly observed in the physical world ([36]). In the past few decades, many researchers have investigated the emergence of patterns by using self-diffusion in reaction–diffusion systems [18,20,24,35,36]. Nowadays, the highlighted topic in the field of dynamical systems is the effect of cross-diffusion on the emergence of patterns, and it has been found that with linear reaction terms, appropriate cross-diffusion coefficients are sufficient to produce the patterns [1,26,29]. So far, only a few attention has been paid to the study of the effect of cross-diffusion. In view of these aforementioned motivations, our aim in this paper is to study the formation of patterns in the predator–prey system with the Allee effect with cross-diffusion. More precisely, consider a system

$$\begin{aligned}\frac{\partial u}{\partial t} &= \nabla\cdot\mathbf{J}_1 + \gamma u(u-\beta)(1-u) - uv\\ \frac{\partial v}{\partial t} &= \nabla\cdot\mathbf{J}_2 + uv - \delta v,\end{aligned} \tag{1}$$

where, a_1 and a_2 are the self-diffusion coefficients and b_1 and b are the cross-diffusion coefficients, which may be zero, negative or positive. The term with negative cross-diffusion coefficient represents the fact that one species tends to diffuse in the direction of another species of higher concentration. The positive cross-diffusion coefficient represents the species movement in the direction of another species of lower concentration. In this work, we assume that the cross-diffusion coefficients b_1 and b are both non-negative constants. Here, $0<\beta<1$ corresponds to the strong Allee effect, the parameter $\gamma>0$ and $\delta>0$. $\mathbf{J}_i$ $(i=1,2)$ is the flux and obeys non-linear equations as follows:

$$\begin{aligned}\mathbf{J}_1 &= \nabla[u(a_1u+b_1v)]\\ \mathbf{J}_2 &= \nabla[v(a_2v+bu)].\end{aligned} \tag{2}$$

Here $u\equiv u(x,t)$ and $v\equiv v(x,t)$ are the population densities of prey and predator, respectively at time t and $x\in\Omega$ with $\Omega=[0,L_x]\times[0,L_y]$. For the system (1), Neumann's boundary conditions are:

$$n\cdot\mathbf{J}_1 = n\cdot\mathbf{J}_2 = 0 \quad \text{when } x\in\partial\Omega.$$

The main aim of the paper is to describe the mechanisms of emergence of patterns for the system (1) in the 2D domain with homogeneous Neumann boundary conditions. The vital difference with the one-dimensional case is the possibility that the bifurcation curve appears via simple or multiple eigenvalues, the 1D case is discussed in [21]. A weakly nonlinear analysis is performed close to the bifurcation state by using the multiple scaling analysis, which rules the evolution of the amplitude of patterns near the threshold. The comparison among various methods of a weakly non-linear analysis for some reaction–diffusion models is studied in [34].

A weakly non-linear multiple scale is used to investigate the amplitude and the pattern of forms, which are closed to the bifurcation threshold. In particular, when the homogeneous steady state bifurcates to spatial patterns at a simple eigenvalue, we derive the cubic and quintic Stuart–Landau equation that rules the evolution of the amplitude of the most unstable mode in the supercritical and subcritical cases, respectively. Square and roll patterns are given for these cases [9]. On the contrary, most complex patterns came into existence when double eigenvalues are taken, hexagonal patterns are a particular type of mixed-mode patterns, arises for resonance condition.

Bi-stability and hysteresis occurs, the hexagonal patterns of the amplitudes of evaluation system proved that. For all the cases under consideration, the solutions to non-linear analysis by comparing with numeric values of the original system are close to the threshold.

By degenerating eigenvalues, Turning bifurcation occurs and the mathematical study involves for it, gives a huge variety of patterns, taken as the steady-state solution to the reaction–diffusion system. These are the super squares and the hexagon among the rolls, mixed-mode pattern and square.

The reaction–diffusion system close to instability helps us to obtain the amplitude equations (Stuart–Landau equations). On analyzing the different patterns of amplitude equations, many phenomena occur, such as stable solution leading to hysteresis and stable subcritical Turning pattern. For specific cases, supercritical and subcritical bifurcation gives hexagonal mode and rolls, respectively. Therefore, there is a region of bi-stability where both rolls and hexagons are stable; however, here rolls appear as a transient state due to a spatially modulated cross-roll instability that drives the solution toward a mixed-mode pattern [9]. We achieve partial success in explaining instability due to mode competition.

The organization of this paper is as follows: In Section 2, the stability analysis of the local equilibrium point of system (1) is performed and derived, so that cross-diffusion is responsible for the initiation of the emergence of Turing patterns. In Section 3, by using a weakly non-linear multiple scale analysis, the amplitude and the form of the patterns close to the bifurcation threshold are investigated. When the homogeneous steady state bifurcates to spatial patterns at a simple eigenvalue, the cubic and quintic Stuart–Landau equations are derived, which rule the evolution of the amplitude of the most unstable mode in the supercritical and subcritical case, respectively.

The complete calculation of the weakly nonlinear stability analysis is presented in the Appendix.

2. Cross-diffusion-driven instability

In this section, we will examine the probability of the emergence of patterns for systems (1) and (2). We know that, if the system is stable for the solution to the reaction–diffusion system, then the steady-state system is transformed into an unstable one, i.e. has no diffusion terms, but the reaction–diffusion model solution is unstable. In section 2.1, through linear stability analysis, we will establish the critical wave number and critical value for the bifurcation parameter. The role of the boundary conditions and geometry of the domain is ignored in this process.

In 2.2, we will consider this role to derive the range of unstable wave numbers of permissible patterns scathingly depends on the geometry of dominion. This situation is much more involved in the 1D domain taken in ([21]), as dissipation can happen.

2.1. Main results on the destabilization mechanism

First, by noticing that $0 < \beta < 1$, one obtains that systems (1) and (2) have a unique spatially uniform positive equilibrium

We investigate the conditions, for reaction systems (1) and (2), under which the interior equilibrium is stable, but the reaction–diffusion systems (1) and (2) are unstable.

Firstly, a distinctive spatially uniform positive equilibrium for systems (1) and (2) is obtained, by noticing that $0 < \beta < 1$.

$$E_*(u_0, v_0) = (\delta, \gamma(\delta - \beta)(1 - \delta)),$$

if $\beta < \delta < 1$. Further, it is stable if

$$(C1) : \frac{\beta + 1}{2} < \delta < 1.$$

In the remaining part of this paper, we will always consider that (C1) holds. Now, the linearization of (1) and (2) at $E_*(u_0, v_0)$ is

$$\dot{\mathbf{w}} = K\mathbf{w} + D\nabla^2\mathbf{w}, \quad \mathbf{w} = \begin{pmatrix} u - u_0 \\ v - v_0 \end{pmatrix} \tag{3}$$

where

$$K = \begin{pmatrix} -\gamma u_0[2u_0 - (\beta + 1)] & -u_0 \\ v_0 & 0 \end{pmatrix}, \quad D = \begin{pmatrix} 2a_1u_0 + b_1v_0 & b_1u_0 \\ bv_0 & 2a_2v_0 + bu_0 \end{pmatrix}. \tag{4}$$

The following dispersion relation is obtained by considering the solution to system (3) in the form of $e^{ikx+\lambda t}$, where $k \geq 0$ is the wave number.

$$\lambda^2 + [k^2 \operatorname{tr}(D) - \operatorname{tr}(K)]\lambda + h(k^2) = 0, \tag{5}$$

where

$$h(k^2) = \det(D)k^4 + qk^2 + \det(k), \tag{6}$$

with

$$q = 2a_2\gamma u_0v_0[2u_0 - (\beta + 1)] + b_1u_0v_0 + bu_0[\gamma u_0(2u_0 - \beta - 1) - v_0]. \tag{7}$$

For having Turning instability and formation of spatial patterns, it is obvious from (5) that there should be a $k \neq 0$ such that, for the characteristic equation (5), there must be at least one root greater than zero, i.e. $Re(\lambda) > 0$; condition (C1) implies that

$$k^2 \operatorname{tr}(D) - \operatorname{tr}(K) > 0, \quad \forall\, k \neq 0.$$

When $h(k^2) < 0$, the existence of $k > 0$ is equivalent to the existence of λ, so that $Re(\lambda) > 0$.

Next, we will derive the critical wave number, critical values of bifurcation occurrence, and also the conditions implying the emergence of spatial patterns. Since $h(k^2)$ in terms of k^2 and $\det(D) > 0$, is the quadratic equation. Now, the condition for the marginal stability from (6) can be obtained as follows,

$$\min(h(k^2)) = 0, \tag{8}$$

where

$$k_c^2 = -\frac{q}{2\det(D)}, \tag{9}$$

which requires $q < 0$. In the present study, the presence of the cross-diffusion term $b > 0$ yields the potential destabilizing mechanism, while in the previous studies [35,36] the spatial uniform equilibrium is destabilized due to self-diffusion. If the cross-diffusion effect is zero ($b = 0$), due to the condition C1 the term q in (7) is positive. The term q in (7) in negative, when $b > 0$, which implies

$$3\delta^2 - 2(\beta + 1)\delta + \beta < 0. \tag{10}$$

For the emergence of patterns, the above condition is the necessary condition. We seek for a critical value at which bifurcation occurs by using the cross-diffusion coefficient b and as the bifurcation parameter, which defines

$$\tilde{\alpha} = u_0[v_0 - \gamma u_0(2u_0 - \beta - 1)], \quad \tilde{\beta} = 2a_2\gamma u_0 v_0[2u_0 - (\beta + 1)] + b_1 u_0 v_0,$$

and let $b = \frac{\tilde{\beta}}{\tilde{\alpha}} + \xi$. After substituting b into (8), one can obtain the expression for ξ

$$\frac{\tilde{\alpha}^2}{4\det(K)}\xi^2 - 2a_1 u_0^2 \xi - [\frac{\tilde{\beta}}{\tilde{\alpha}} \cdot 2a_1 u_0^2 + 2a_2 v_0(2a_1 u_0 + b_1 v_0)] = 0. \tag{11}$$

Let ξ^+ be the positive root of (11); then the value of critical bifurcation is given by:

$$b^c = \frac{\tilde{\beta}}{\tilde{\alpha}} + \xi^+. \tag{12}$$

The above analysis is summarized by the following theorem.

Theorem 2.1. *Let (C1) and (10) hold, then the interior equilibrium point $E_*(u_0, v_0)$ of equation systems (1) and (2) is unstable when $b > b^c$, where b^c is represented as in (12).*

Remark 2.2. In Fig. 1, we show in $\beta - \delta$ plane the region satisfied by conditions (C1) and (10), see the shaded region, which is bounded by the straight line $\delta = \frac{\beta+1}{2}$ above and by curve $3\delta^2 - 2(\beta + 1)\delta + \beta = 0$ below and gives the parameter space where the spatial patterns may form. Noticing that β stands for the Allee effect and δ for the predator mortality rate, in order to admit the formation of spatial patterns, a lower Allee effect allows a larger range of predator mortality rates, and a higher Allee effect allows a smaller range, but a larger predator mortality rate.

2.2. Instability bands and degeneracy

When the domain is finite, the condition $b > b^c$ is not enough to see a pattern emerging. In this case, in fact, k^c might not be a mode admissible for the domain and the boundary condition. However, when $b > b^c$, there exists a range (k_1^2, k_2^2) of unstable wavenumbers such that $h(k^2) < 0$ and, correspondingly, $Re(\lambda) > 0$, see Fig. 2. It is easy to see that the extremes of the interval of unstable wavenumbers, k_1^2 and k_2^2, where $h(k^2) = 0$. It follows that at least one of the modes allowed by the Neumann boundary conditions within the interval $[k_1^2, k_2^2]$.

In a rectangular domain defined by $0 < x < L_x$ and $0 < y < L_y$, the solutions to the linear system (3) with Neumann boundary conditions are:

$$\mathbf{w} = \sum_{m,n\in\mathbb{N}} \mathbf{f}_{mn} e^{\lambda(k_{mn}^2)t} \cos\left(\frac{m\pi}{L_x}x\right)\cos\left(\frac{n\pi}{L_y}y\right), \tag{13}$$

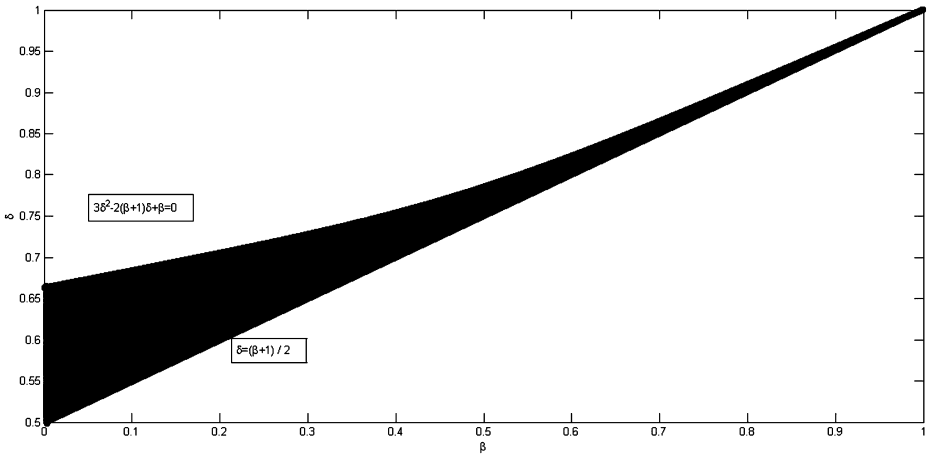

Fig. 1. Allee effect β vs. predator mortality rate δ: the bounded area shows the parameter space where Turing instabilities may occur.

$$k_{mn}^2 = \left(\frac{m\pi}{L_x}\right)^2 + \left(\frac{n\pi}{L_y}\right)^2, \tag{14}$$

where $\mathbf{f}_{m,n}$ are the Fourier coefficients of the initial conditions; the values $\lambda(k_{mn}^2)$ are derived from the dispersion relation (5). The occurrence of a pattern emerging as t increases, therefore depends on the existence of mode pairs (m, n) such that:

$$k_1^2 < k^2 \equiv \phi^2 + \psi^2 < k_2^2, \quad \text{where } \phi \equiv \frac{m\pi}{L_x}, \ \psi \equiv \frac{n\pi}{L_y}, \tag{15}$$

$$\lambda(k^2) > 0, \tag{16}$$

i.e. for $b > b^c$. In what follows, we shall restrict ourselves to the case when there is only one unstable eigenvalue, admissible for the Neumann boundary conditions, that falls within the band (k_1, k_2) in the sense of Eq. (15). We shall denote this admissible eigenvalue with $\bar{k_c}$ to distinguish from the critical value k_c. In a two-dimensional domain, given $\bar{k_c} \in [k_1, k_2]$, one, two or more pairs (m, n) may exist such that the condition

$$\bar{k_c}^2 = \phi^2 + \psi^2 = \left(\frac{m\pi}{L_x}\right)^2 + \left(\frac{n\pi}{L_y}\right)^2, \tag{17}$$

is satisfied and, in this case, the eigenvalue λ will have single, double or higher multiplicity respectively. The multiplicity of the eigenvalue, and therefore the type of linear patterns we could expect, strictly depends on the dimensions of the domain L_x and L_y.

Remark 2.3. It can be easily verified that $k^2\,\mathrm{tr}(D) - \mathrm{tr}(K)$ is positive. We consider b as the parameter of bifurcation and the Turing bifurcation threshold for $k \equiv k^c$ at $b = b^c$ such that $\min(h(k^2)) = 0$.

To understand the diffusion-driven instability conditions, Fig. 2 is provided. The pink, brown, and green curves in Fig. 2 tell that the real part of the eigenvalue λ is negative for the parametric values $\gamma = 6$, $\beta = 0.6$, $\delta = 0.81$, $a_1 = 0.1$, $a_2 = 0.1$ and $b_1 = 0.01$, which shows that the homogenous steady state is stable for heterogenous perturbations. The corresponding curves (blue, black) of Fig. 2 tells that the real part of the eigenvalue λ is positive for a certain interval of $|k|$ at which the model becomes unstable to heterogenous perturbations and produces Turing patterns, when $b > b^c$ is considered. Similarly, in Fig. 3, the black, light green and brown curves show that $h(k^2) > 0$, which shows that the homogenous steady state is stable for heterogenous perturbations. The corresponding curves (dark green, blue) of Fig. 3 tell that $h(k^2) < 0$ for a certain interval of $|k|$ at which the model becomes unstable to heterogenous perturbations and produces Turing patterns, when $b > b^c$ is considered. However, we cannot determine the Turing patterns selection. Next, we will obtain the amplitude equations of Turing patterns near the onset $b = b^c$, which explains the stability of different kinds of Turing patterns as well as the structural transitions between them.

3. Weakly nonlinear analysis

This section deals with weakly nonlinear analysis. This analysis is conducted to find the amplitude equations that explain the dynamics close to the critical bifurcation state. Newell [16] has introduced the multiple-scale method along with the asymptotic analysis of the model that is close to its marginal stability. This method is employed to attain the critical bifurcation dynamics of the patterns [7].

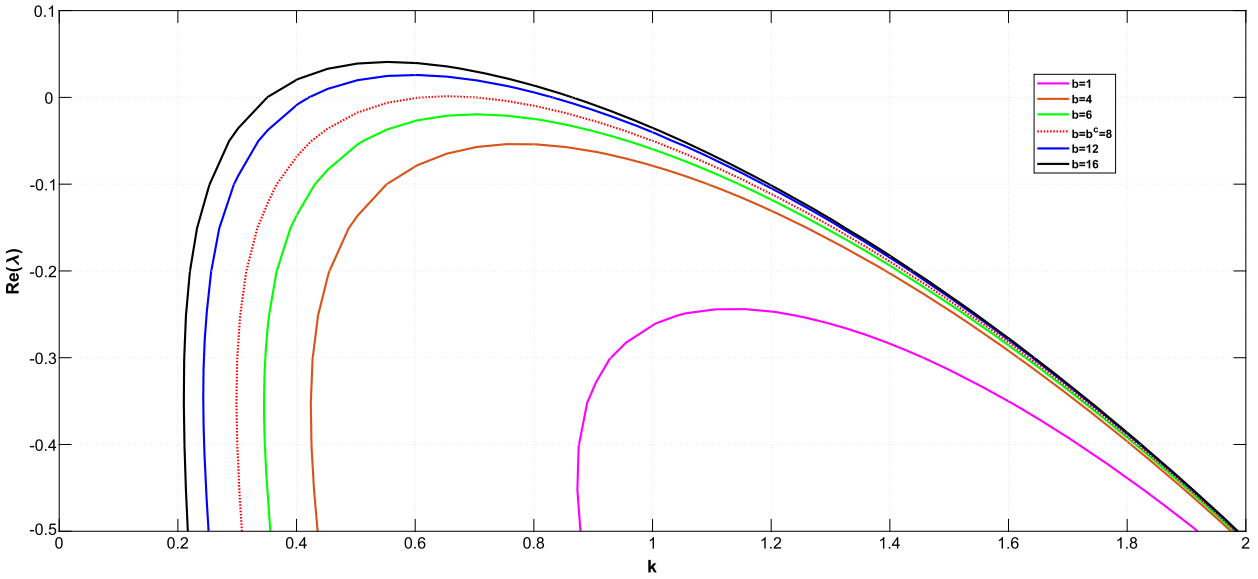

Fig. 2. Different dispersion relations of system (1).

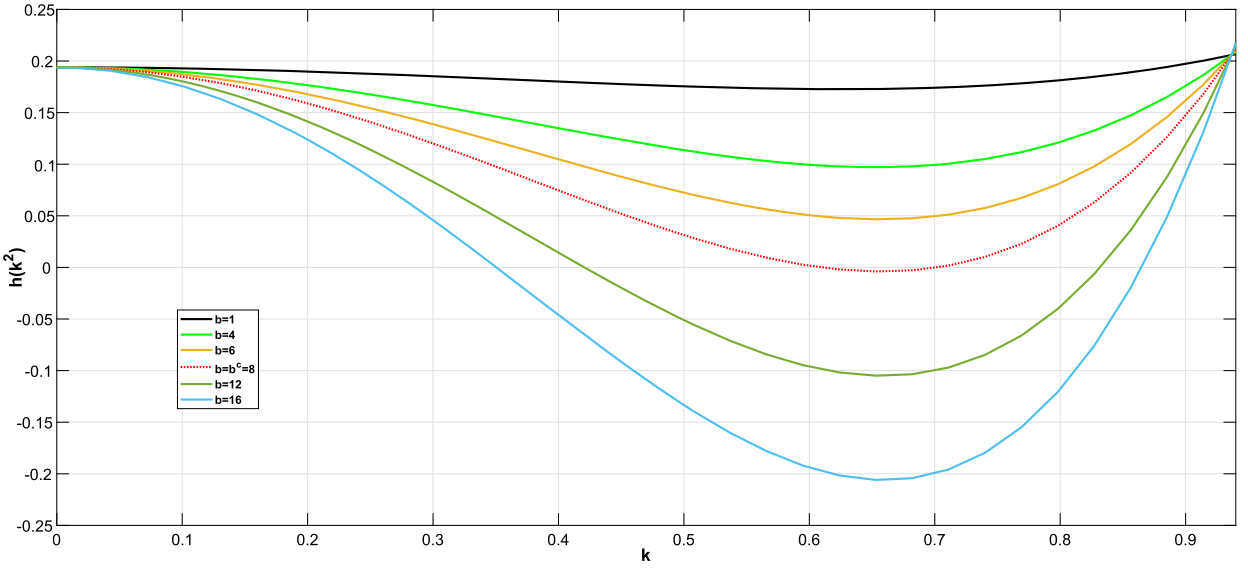

Fig. 3. Plot of $h(k^2)$ for different values of b while setting other parameters as $\gamma = 6$, $\beta = 0.6$, $\delta = 0.81$, $a_1 = 0.1$, $a_2 = 0.1$ and $b_1 = 0.01$.

The amplitude of the patterns evolves close to the threshold based on a slow temporal scale. For this reason, we will introduce the scale coordinate that divides the time into two parts, i.e. $T = \epsilon t$ is the slow time and t is a fast time, respectively, where ϵ is the control parameter that is used to measure the distance from bifurcation, as shown in (22).

The solution to model (1) can be expressed as an expansion of ϵ. In addition, the leading-order term can be written as a product of the basic pattern and of a gradually changing amplitude (for details, see [12,33]). We will restrict our analysis to patterns that are based on time instead of space. Hence, we will not consider the slow spatial scale.

The linear operator can be defined as:

$$\mathbf{L}^b = K + D^b \nabla^2, \tag{18}$$

where K and D^b are shown in (4). The bilinear operators based on (x, y) with $x \equiv (x^u, x^v)$ and $y \equiv (y^u, y^v)$*are*:

$$\mathcal{Q}_K(x, y) = \begin{pmatrix} 2\gamma(\beta+1)x^u y^u - (x^u y^v + x^v y^u) \\ x^u y^v + x^v y^u \end{pmatrix}, \tag{19}$$

$$\mathcal{Q}_D^b(x, y) = \begin{pmatrix} 2a_1 x^u y^u + b_1(x^u y^v + x^v y^u) \\ 2a_2 x^v y^v + b(x^u y^v + x^v y^u) \end{pmatrix}. \tag{20}$$

Hence, system (1) can be expressed as:

$$\partial_t \mathbf{w} = \mathbf{L}^b \mathbf{w} + \frac{1}{2}\mathcal{Q}_K(\mathbf{w},\mathbf{w}) + \frac{1}{2}\mathcal{Q}_D^b(\mathbf{w},\mathbf{w}) + \begin{pmatrix} -\gamma(u-u_0)^3 \\ 0 \end{pmatrix}, \tag{21}$$

where $\mathbf{w}$ is given in (3).

Now, the multiple time scales are introduced by:

$$t = \frac{T_1}{\epsilon} + \frac{T_2}{\epsilon^2} + \frac{T_3}{\epsilon^3} + \frac{T_4}{\epsilon^4} + \cdots. \tag{22}$$

The bifurcation parameter b and the solution $\mathbf{w}$ can be expanded as:

$$\mathbf{w} = \epsilon\mathbf{w}_1 + \epsilon^2\mathbf{w}_2 + \epsilon^3\mathbf{w}_3 + \epsilon^4\mathbf{w}_4 + \mathcal{O}(\epsilon^5), \tag{23}$$

$$b = b^{\mathrm{c}} + \epsilon b^{(1)} + \epsilon^2 b^{(2)} + \epsilon^3 b^{(3)} + \epsilon^4 b^{(4)} + \mathcal{O}(\epsilon^5). \tag{24}$$

Here, the smallness parameter is defined by expansion (24). Now onward, the critical value b^{c} is used to measure the threshold distance. This implies that, if $b^{\mathrm{c}} \neq 0$, then $b^{(i)} = b^{\mathrm{c}}$. The linear expression for $\mathbf{w}_i$ can be obtained by substituting (22)–(24) into (1).

$$\mathcal{O}(\varepsilon) : \mathbf{L}^{b^{\mathrm{c}}}\mathbf{w}_1 = 0, \tag{25}$$

$$\mathcal{O}(\varepsilon^2) : \mathbf{L}^{b^{\mathrm{c}}}\mathbf{w}_2 = \mathbf{F} = \frac{\partial \mathbf{w}_1}{\partial T_1} - \frac{1}{2}\Big(\mathcal{Q}_K + \nabla^2\mathcal{Q}_D^{b^{\mathrm{c}}}\Big)(\mathbf{w}_1,\mathbf{w}_1) - b^{(1)}\begin{pmatrix} 0 & 0 \\ v_0 & u_0 \end{pmatrix}\nabla^2\mathbf{w}_1, \tag{26}$$

$$\begin{aligned}\mathcal{O}(\varepsilon^3) : \mathbf{L}^{b^{\mathrm{c}}}\mathbf{w}_3 = \mathbf{G} = {} & \frac{\partial \mathbf{w}_1}{\partial T_2} + \frac{\partial \mathbf{w}_2}{\partial T_1} - \Big(\mathcal{Q}_K + \nabla^2\mathcal{Q}_D^{b^{\mathrm{c}}}\Big)(\mathbf{w}_1,\mathbf{w}_2) - b^{(1)}\nabla^2\begin{pmatrix} 0 \\ \mathbf{w}_1^u\mathbf{w}_1^v \end{pmatrix} \\ & - \begin{pmatrix} 0 & 0 \\ v_0 & u_0 \end{pmatrix}\big(b^{(1)}\nabla^2\mathbf{w}_2 + b^{(2)}\nabla^2\mathbf{w}_1\big) + \begin{pmatrix} \gamma(\mathbf{w}_1^u)^3 \\ 0 \end{pmatrix},\end{aligned} \tag{27}$$

$$\begin{aligned}\mathcal{O}(\varepsilon^4) : \mathbf{L}^{b^{\mathrm{c}}}\mathbf{w}_4 = \mathbf{H} = {} & \frac{\partial \mathbf{w}_1}{\partial T_3} + \frac{\partial \mathbf{w}_2}{\partial T_2} + \frac{\partial \mathbf{w}_3}{\partial T_1} - \Big(\mathcal{Q}_K + \nabla^2\mathcal{Q}_D^{b^{\mathrm{c}}}\Big)(\mathbf{w}_1,\mathbf{w}_3) - b^{(2)}\nabla^2\begin{pmatrix} 0 \\ \mathbf{w}_1^u\mathbf{w}_1^v \end{pmatrix} \\ & - \frac{1}{2}\Big(\mathcal{Q}_K + \nabla^2\mathcal{Q}_D^{b^{\mathrm{c}}}\Big)(\mathbf{w}_2,\mathbf{w}_2) - b^{(1)}\nabla^2\begin{pmatrix} 0 \\ \mathbf{w}_1^u\mathbf{w}_2^v + \mathbf{w}_2^u\mathbf{w}_1^v \end{pmatrix} \\ & - \begin{pmatrix} 0 & 0 \\ v_0 & u_0 \end{pmatrix}\big(b^{(1)}\nabla^2\mathbf{w}_3 + b^{(2)}\nabla^2\mathbf{w}_2 + b^{(3)}\nabla^2\mathbf{w}_1\big) + \begin{pmatrix} 3\gamma(\mathbf{w}_1^u)^2\mathbf{w}_2^u \\ 0 \end{pmatrix},\end{aligned} \tag{28}$$

$$\begin{aligned}\mathcal{O}(\varepsilon^5) : \mathbf{L}^{b^{\mathrm{c}}}\mathbf{w}_5 = \mathbf{P} = {} & \frac{\partial \mathbf{w}_1}{\partial T_4} + \frac{\partial \mathbf{w}_2}{\partial T_3} + \frac{\partial \mathbf{w}_3}{\partial T_2} + \frac{\partial \mathbf{w}_4}{\partial T_1} - \Big(\mathcal{Q}_K + \nabla^2\mathcal{Q}_D^{b^{\mathrm{c}}}\Big)(\mathbf{w}_1,\mathbf{w}_4) \\ & - \Big(\mathcal{Q}_K + \nabla^2\mathcal{Q}_D^{b^{\mathrm{c}}}\Big)(\mathbf{w}_2,\mathbf{w}_3) - \begin{pmatrix} 0 & 0 \\ v_0 & u_0 \end{pmatrix}\big(b^{(1)}\nabla^2\mathbf{w}_4 + b^{(2)}\nabla^2\mathbf{w}_3 \\ & + b^{(3)}\nabla^2\mathbf{w}_2 + b^{(4)}\nabla^2\mathbf{w}_1\big) - b^{(1)}\nabla^2\begin{pmatrix} 0 \\ \mathbf{w}_1^u\mathbf{w}_3^v + \mathbf{w}_2^u\mathbf{w}_2^v + \mathbf{w}_3^u\mathbf{w}_1^v \end{pmatrix} \\ & - b^{(2)}\nabla^2\begin{pmatrix} 0 \\ \mathbf{w}_1^u\mathbf{w}_2^v + \mathbf{w}_2^u\mathbf{w}_1^v \end{pmatrix} - b^{(3)}\nabla^2\begin{pmatrix} 0 \\ \mathbf{w}_1^u\mathbf{w}_1^v \end{pmatrix} \\ & + \begin{pmatrix} 3\gamma[(\mathbf{w}_1^u)^2\mathbf{w}_3^u + \mathbf{w}_1^u(\mathbf{w}_2^u)^2] \\ 0 \end{pmatrix}.\end{aligned} \tag{29}$$

The problem (25) hold the Neumann boundary conditions and the solution is represented by:

$$\mathbf{w}_1 = \sum_{i=1}^{m} A_i(T_1,T_2)\boldsymbol{\rho}\cos(\phi_i x)\cos(\psi_i y), \tag{30}$$

where m denotes the multiplicity of the eigenvalue, A_i represents the gradually changing amplitudes, while $\boldsymbol{\rho}$ is defined to be a constant and can be explicitly expressed by:

$$\boldsymbol{\rho} \in \ker(K - k_{\mathrm{c}}^2 D^{b^{\mathrm{c}}}), \quad \boldsymbol{\rho} = \begin{pmatrix} 1 \\ M \end{pmatrix}, \quad \text{with } M \equiv \frac{-D_{21}^{b^{\mathrm{c}}}k_{\mathrm{c}}^2 + K_{21}}{D_{22}^{b^{\mathrm{c}}}k_{\mathrm{c}}^2 - K_{22}}, \tag{31}$$

where $D_{ij}^{b^{\mathrm{c}}}$ and K_{ij} are the i, j-entries of the matrices $D^{b^{\mathrm{c}}}$ and K.

However, we will restrict the multiplicity to $m = 1$.

3.1. Simple eigenvalue, $m = 1$

For the simple eigenvalue, $m = 1$, the solution (30) reduces to

$$\mathbf{w}_1 = A(T_1, T_2)\boldsymbol{\rho}\cos(\phi_i x)\cos(\psi_i y). \tag{32}$$

Substituting this expression into the linear equation (26), the vector $\mathbf{F}$ is made orthogonal to the kernel of the adjoint of $\mathbf{L}^{b^c}$ simply by imposing $T_1 = 0$ and $b^{(1)} = 0$; see the details in Appendix A.1.

Substitute the above equation into (26) and let $T_1 = 0$, $b^{(1)} = 0$ then the vector $\mathbf{F}$ is orthogonal to the kernel of adjoint of $\mathbf{L}^{b^c}$. For details, see Appendix A.1. The solution to (26) can be derived (see (39) and substituted at order ε^3 in (27). The $\mathbf{G}$ vector contains the secular terms, represented in (41). By using Fredholm's solvability condition, the cubic Stuart–Landau equation is obtained for the amplitude $A(T_2)$:

$$\frac{\mathrm{d}A}{\mathrm{d}T_2} = \sigma A - LA^3. \tag{33}$$

The expressions for σ and L are given in (42) in terms of the parameters of original reaction–diffusion model (1).

Since, the coefficient of $\sigma > 0$ and the Landau constant L is either negative or positive, depending on the parametric values of the model. According to the Landau constant sign, we deduce the following bifurcation direction:

- the detailed analysis is given in (3.1.1) for the supercritical bifurcation, when $L > 0$;
- for a subcritical bifurcation, when $L < 0$, Eq. (33) is not sufficient and we need higher orders. For this, the detailed analysis is given in (3.1.2).

3.1.1. The supercritical case

In the supercritical case, both coefficients $(\sigma, L) > 0$. In this case, since the coefficients σ and L are both positive, the solution to the Stuart–Landau equation changes to the stable stationary state $A_\infty = \sqrt{\frac{\sigma}{L}}$. Further, when b passes b^c, we assume that $\bar{k_c}$ be the first integer, so that A_∞ becomes unstable. The above analysis can be summarized by the following theorem.

Theorem 3.1. *Assume that:*

1) $\epsilon^2 = \frac{b-b^c}{b^c}$ *is small enough that the uniform steady state* (u_0, v_0) *of (1) is unstable for modes corresponding only to the eigenvalue* $\bar{k_c}$*, which is stated as above;*
2) *there exists only one couple of integers* (m, n) *such that:* $\bar{k_c}^2 \equiv \phi^2 + \psi^2$ *where* $\phi \equiv \frac{m\pi}{L_x}$, $\psi \equiv \frac{n\pi}{L_y}$,
3) *the Landau coefficient* $L > 0$ *in (42).*

Then the emerging solution to model (1) is represented by:

$$\mathbf{w} = \epsilon\rho A_\infty \cos(\phi x)\cos(\psi y) + O(\epsilon^2) \tag{34}$$

where A_∞ *is the stable stationary state of the Stuart–Landau equation (33), and* ρ *is given in (31).*

3.1.2. The subcritical case

For specific values of parameters, L (Landau constant) takes a negative value. This is an average case, where the transition happens by means of a subcritical bifurcation. Clearly for this situation, Eq. (33) cannot capture the amplitude of the pattern. In order to foresee the amplitude of the pattern, weakly nonlinear expansions should be extended to higher order (for details see [2]).

Hence, the quintic Stuart–Landau equation for amplitude A can be obtained by performing a weakly nonlinear analysis up to $O(\epsilon^5)$:

$$\frac{\mathrm{d}A}{\mathrm{d}T_2} = \bar{\sigma} A - \bar{L}A^3 + \bar{Q}A^5. \tag{35}$$

For details, see Appendix A.1.1. Hence, we can summarize the results of our WNL analysis in non-degenerate subcritical case as follows.

WNL analysis results in the non-degenerate subcritical case.

Let suppose that Theorem (3.1), the hypotheses *(1)* and *(2)* hold.

4) L in (42) is negative;
5) the coefficient $\bar{Q}$, presented in (48) is positive.

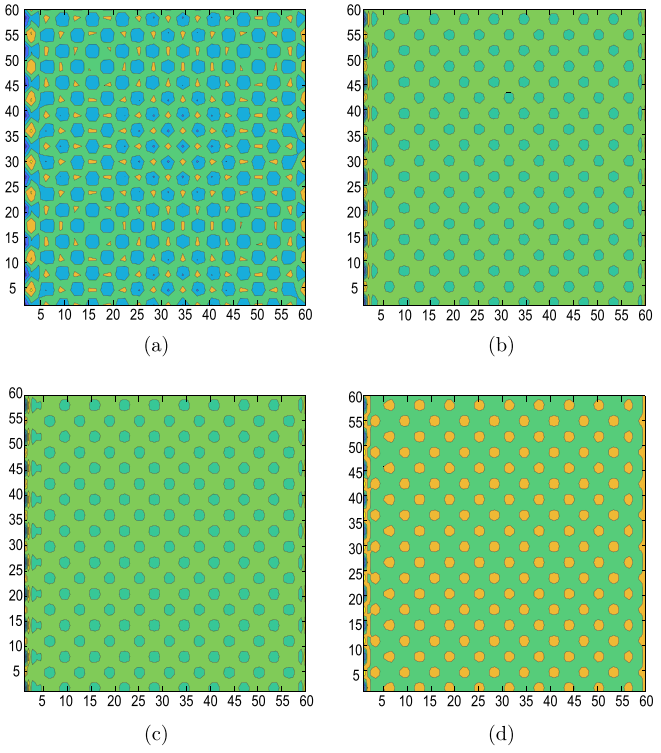

Fig. 4. Hexagonal patterns occur.

Hence, the solution to our model (1) is represented by:

$$\mathbf{w} = \epsilon\rho A_\infty \cos(\phi x)\cos(\psi y) + O(\epsilon), \tag{36}$$

where ρ is defined in equation (31) and A_∞ is the stable stationary state of Eq. (33).

It is vital to see that the coefficient $\bar{Q} = O(\epsilon^2)$. While $\bar{\sigma}$ and $\bar{L}$ are $O(1)$ as it is obvious from (48), one the equilibrium $A_\infty = O(\epsilon^{-1})$.

4. Numerical simulation

A numerical simulation is presented to explain the theoretical analysis. In this paper, we use the fractional exponential integrator scheme [5,13,19,30] to test our numerical method with a space fractional reaction–diffusion model. Furthermore, to assure that Turing patterns are generated, boundary conditions are chosen in the spatial domain in our simulation. All simulation run for $N = 60$. The mathematical software Matlab (2014a) is used to plot the numerical graphs.

Hexagonal patterns exist by choosing the parameters as $\gamma = 6$, $\beta = 0.6$, $\delta = 0.81$, $a_1 = 0.1$, $a_2 = 0.1$, $b_1 = 0.01$ and $b = 8.5$ with initial perturbation $u = 0.2 + 0.01\sin(Y)\cos(X)$, $v = 0.2 + 0.01\sin(X)\cos(Y)$ with the number of iterations (a) $T = 40$, (b) $T = 64$, (c) $T = 68$, and (d) $T = 72$ (see Fig. 4).

Spot patterns exist by choosing the parameters as $\gamma = 8$, $\beta = 0.2$, $\delta = 0.65$, $a_1 = 0.1$, $a_2 = 0.1$, $b_1 = 0.01$ and $b = 16$ with initial perturbation $u = 0.1 + 0.05\sin(X)\cos(Y) + 0.05\cos(Y)$, $v = 0.1 + 0.05\sin(Y)\cos(X) + 0.05\cos(X)$ with the number of iterations (a) $T = 64$, (b) $T = 128$, (c) $T = 232$, and (d) $T = 280$ (see Fig. 5).

Square and spot patterns exist by choosing the parameters as $\gamma = 7$, $\beta = 0.2$, $\delta = 0.65$, $a_1 = 0.1$, $a_2 = 0.1$, $b_1 = 0.01$ and $b = 15$, with initial perturbation $u = 0.1 + 0.05\sin(X)\cos(Y) + 0.05\cos(Y)$, $v = 0.1 + 0.05\sin(Y)\cos(X) + 0.05\cos(X)$ with the number of iterations (a) $T = 64$, (b) $T = 128$, (c) $T = 234$, and (d) $T = 280$ (see Fig. 6).

Square patterns exist by choosing the parameters as $\gamma = 4$, $\beta = 0.8$, $\delta = 0.9$, $a_1 = 0.1$, $a_2 = 0.1$, $b_1 = 0.01$ and $b = 12$ with initial perturbation $u = 0.5 + 0.01\sin(\frac{Y}{2})\cos(\frac{X}{2})$, $v = 0.05 + 0.03\sin(\frac{X}{2})\cos(\frac{Y}{2})$ with the number of iterations (a) $T = 50$, (b) $T = 60$, (c) $T = 64$ and (d) $T = 68$ (see Fig. 7).

Stripe patterns exist by choosing the parameters as $\gamma = 1$, $\beta = 0.1$, $\delta = 0.6$, $a_1 = 0.1$, $a_2 = 0.1$, $b_1 = 0.01$ and $b = 10$ with initial perturbation $u = 0.01\cos^2(\frac{X}{2})$, $v = 0.03\sin^2(\frac{Y}{2})$ with the number of iterations (a) $T = 30$, (b) $T = 50$, (c) $T = 150$, and (d) $T = 200$ (see Fig. 8).

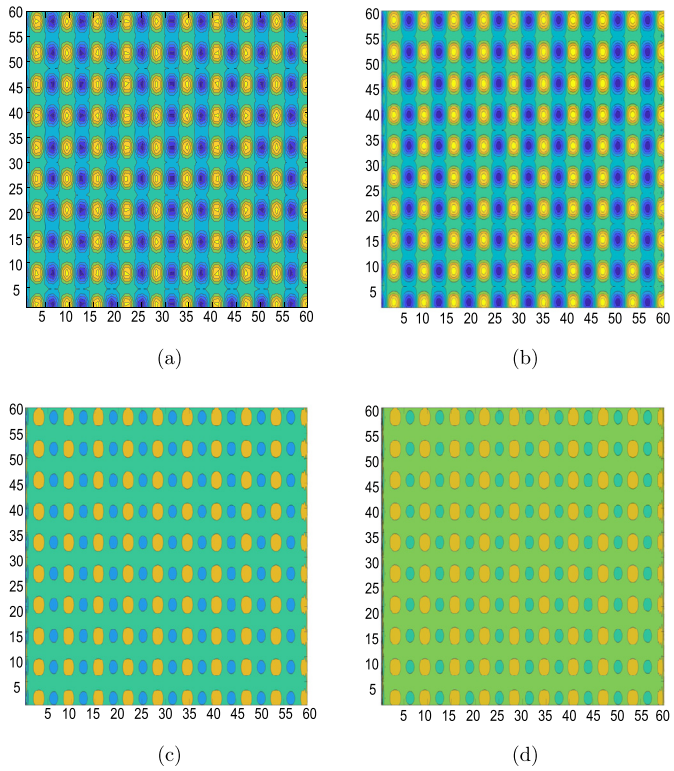

Fig. 5. Spot patterns occur.

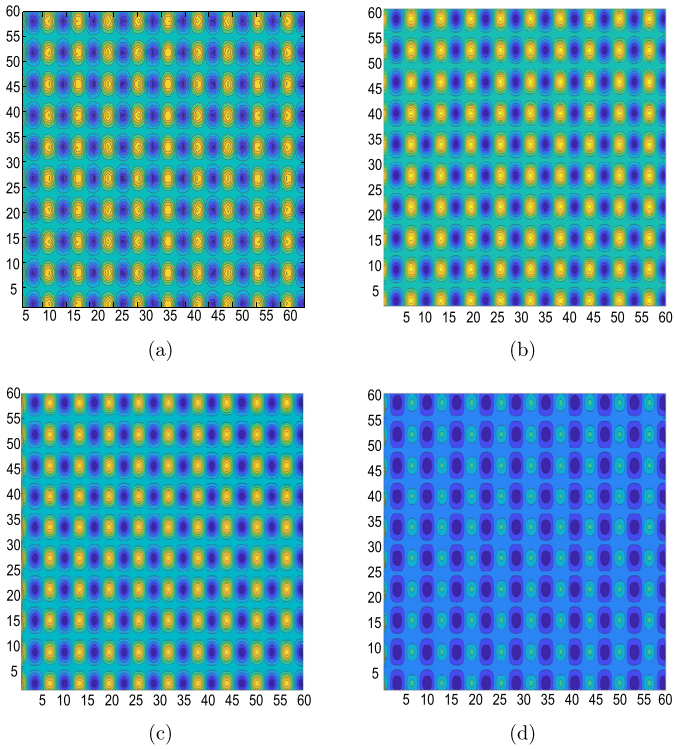

Fig. 6. A mixture of square and spot patterns occurs.

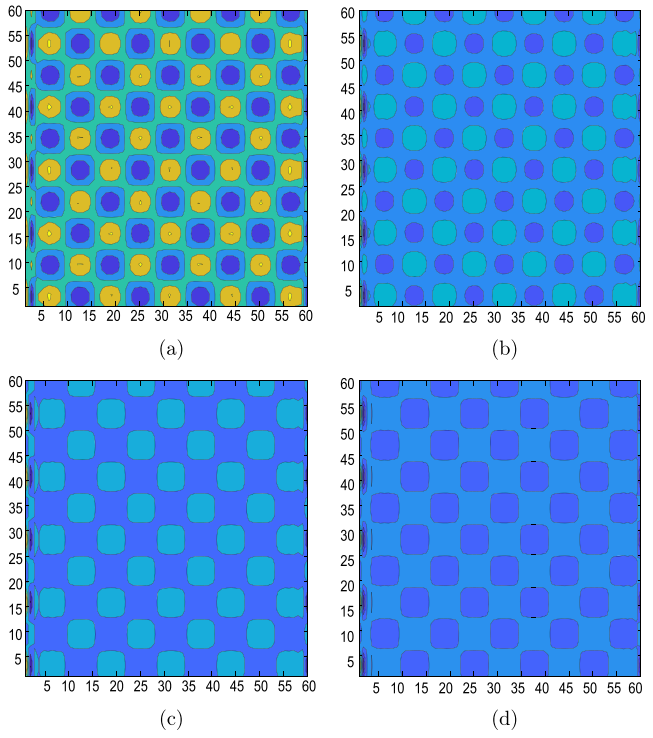

Fig. 7. Square patterns occur.

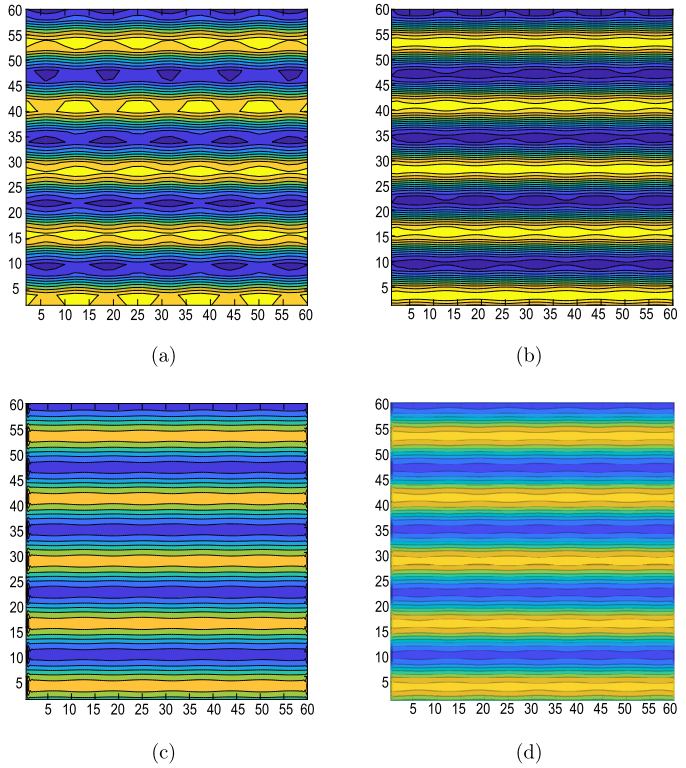

Fig. 8. Stripe patterns occur.

5. Conclusions

This paper deals with the investigation of the Turing mechanism driven by cross-diffusion on a spatial 2D domain with strong Allee effect. By means of stability analysis, some conditions ensure the diffusion-driven instability of the system. So under such conditions, the system will admit Turing instabilities and different kinds of formed patterns. These are hexagons, spots, squares, a mixture of spots and squares, stripes. We have derived the amplitude equations (for the supercritical case, the cubic Stuart–Landau equation, and for subcritical case, the quintic Stuart–Landau equation) for the original model (1) near the onset of instability. The addition of cross-diffusion terms produces very accurate patterns.

Acknowledgements

This work was supported by the National Science Foundation of China (No. 11571016, 61403115, 11971032).

Appendix A. WNL (weakly nonlinear) analysis

The detail calculation of the WNL analysis is given in this appendix.

A.1. Simple eigenvalue

F in (26) can be written as:

$$\mathbf{F} = -\frac{1}{8}A_1^2 \sum_{i,j=0\ i,j\neq 1}^{2} \zeta_{ij}^1(\rho,\rho)\cos(i\phi_1 x)\cos(j\psi_1 y) + \left(\frac{\partial A_1}{\partial T_1}\rho + b^{(1)}\bar{k}_c^2 A_1 \begin{pmatrix} 0 \\ u_0 M + v_0 \end{pmatrix}\right)\cos(\phi_1 x)\cos(\psi_1 y), \tag{37}$$

where $\zeta_{ij}^1 = Q_k - (i^2\phi_1^2 + j^2\psi_1^2)Q_D^{b^c}$.

Using Fredholm's solvability condition, Eq. (26) has a solution if and only if $\langle \mathbf{F}, \mathbf{Y}\rangle = 0$. Here, $\langle .,. \rangle$ is the scalar product in $L^2(0, \frac{2\pi}{k_c})$ and the vector $\mathbf{Y} \in \ker(\mathbf{L}^{\mathbf{b^c}})^\dagger$ is given by:

$$\mathbf{Y} = \begin{pmatrix} 1 \\ M^* \end{pmatrix}, \quad M^* = \frac{-D_{12}^{b^c}k_c^2 + K_{12}}{D_{22}^{b^c}k_c^2 - K_{22}}. \tag{38}$$

By this condition, we find an equation for the amplitude $A_1(T_1, T_2)$ of the following form:

$$\frac{\partial A_1}{\partial T_1} = \alpha A_1,$$

where $\alpha = -\frac{b^{(1)}\bar{k}_c^2(u_0M+v_0)}{1+MM^*}$. The above amplitude equation does not indicate anything about the asymptotic behavior of the amplitude of patterns.

Hence, the secular terms presented in **F** can be conquered by imposing $T_1 = 0$ and $b^{(1)} = 0$ and automatically the condition holds. Now, we can calculate the solution to (26) as follows:

$$\mathbf{w}_2 = A_1^2 \sum_{i,j=0\ i,j\neq 1}^{2} \mathbf{w}_{2ij}\cos(i\phi_1 x)\cos(j\psi_1 y), \tag{39}$$

where $\mathbf{w}_{2ij}(i, j = 0, 2(i, j \neq 1))$ are the solutions to the systems:

$$L_{ij}^1 \mathbf{w}_{2ij} = -\frac{1}{8}\zeta_{ij}^1(\rho,\rho), \tag{40}$$

and the operators $L_{ij}^1 = K - (i^2\phi^2 + j^2\psi^2)D^{b^c}$.

At order ϵ, the **G** vector is represented by:

$$\mathbf{G} = \left(\frac{\mathrm{d}A_1}{\mathrm{d}T_2}\rho + A_1\mathbf{G}_{11}^{(1)} + A_1^3\mathbf{G}_{11}^{(3)}\right)\cos(\phi_1 x)\cos(\psi_1 y) + A_1^3\mathbf{G}^*, \tag{41}$$

where the terms of $\mathbf{G}^*$ automatically satisfy the Fredholm solvability condition:

$$\mathbf{G}^* = \mathbf{G}_1^* \cos(3\phi_1 x)\cos(\psi_1 y) + \mathbf{G}_2^* \cos(\phi_1 x)\cos(3\psi_1 y) + \mathbf{G}_3^* \cos(3\phi_1 x)\cos(3\psi_1 y),$$
$$\mathbf{G}_1^* = \begin{pmatrix} \frac{1}{4}\gamma\rho^3 \\ 0 \end{pmatrix} - \frac{1}{2}\zeta_{31}^1\left(\rho, \mathbf{w}_{220} + \frac{1}{2}\mathbf{w}_{220}\right),$$
$$\mathbf{G}_2^* = \begin{pmatrix} \frac{1}{4}\gamma\rho^3 \\ 0 \end{pmatrix} - \frac{1}{2}\zeta_{13}^1\left(\rho, \mathbf{w}_{202} + \frac{1}{2}\mathbf{w}_{222}\right),$$
$$\mathbf{G}_3^* = \begin{pmatrix} \frac{1}{4}\gamma\rho^3 \\ 0 \end{pmatrix} - \frac{1}{4}\zeta_{33}^1\left(\rho, \mathbf{w}_{222}\right).$$

The vectors $\mathbf{G}_{11}^{(1)}$ and $\mathbf{G}_{11}^{(3)}$ read:

$$\mathbf{G}_{11}^{(1)} = b^{(2)}\bar{k}_c^2 \begin{pmatrix} 0 \\ u_0 M + v_0 \end{pmatrix},$$
$$\mathbf{G}_{11}^{(3)} = \begin{pmatrix} \frac{3}{4}\gamma\rho^3 \\ 0 \end{pmatrix} - \zeta_{11}^1\left(\rho, \mathbf{w}_{200} + \frac{1}{2}\mathbf{w}_{202} + \frac{1}{2}\mathbf{w}_{220} + \frac{1}{4}\mathbf{w}_{222}\right).$$

For Eq. (27), the Fredholm solvability condition $\langle \mathbf{G}, \mathbf{Y}\rangle = 0$ leads to the Stuart–Landau equation (33), where the equations for the parameters σ and L are

$$\sigma = -\frac{\langle \mathbf{G}_{11}^{(1)}, \mathbf{Y}\rangle}{\langle \rho, \mathbf{Y}\rangle}, \qquad L = \frac{\langle \mathbf{G}_{11}^{(3)}, \mathbf{Y}\rangle}{\langle \rho, \mathbf{Y}\rangle}. \tag{42}$$

A.1.1. The subcritical case

Now, we will provide the detailed calculation for the quintic Stuart–Landau equation (35).

Substituting (22)–(24) into (21), the resulting equations, up to $O(\epsilon^3)$ are the same as those given in (A.1).

Taking into account that (33) is still satisfied for amplitude A_1, the solvability condition $\langle \mathbf{G}, \mathbf{Y}\rangle = 0$ for (27) holds and the solution is:

$$\mathbf{w}_3 = A_1 \mathbf{w}_{311}^{(1)} + A_1^3 \sum_{i,j=1,3} \mathbf{w}_{3ij}\cos(i\phi_1 x)\cos(j\psi_1 y), \tag{43}$$

where $\mathbf{w}_{3ij}$, $i = 1, 3$, can be calculated by solving the following systems:

$$L_{11}^1 \mathbf{w}_{311}^{(1)} = \mathbf{G}_{11}^{(1)}, \quad L_{11}^1 \mathbf{w}_{311} = \mathbf{G}_{11}^{(3)}$$
$$L_{31}^1 \mathbf{w}_{331} = \mathbf{G}_1^*, \quad L_{13}^1 \mathbf{w}_{313} = \mathbf{G}_2^*, \quad L_{33}^1 \mathbf{w}_{333} = \mathbf{G}_3^*.$$

At $O(\epsilon^4)$, the resulting equation is (28), where:

$$\mathbf{H} = \sum_{i,j=0,2,4} \left(A_1^2 \mathbf{H}_{ij}^{(1)} + A_1^4 \mathbf{H}_{ij}^{(2)}\right)\cos(i\phi_1 x)\cos(j\psi_1 y) + \mathbf{H}_{11}\cos(\phi_1 x)\cos(\psi_1 y), \tag{44}$$

and

$$\mathbf{H}_{00}^{(1)} = 2\sigma \mathbf{w}_{200} - \frac{1}{4}\zeta_{00}^{(1)}(\rho, \mathbf{w}_{311}^{(1)}),$$
$$\mathbf{H}_{00} = \begin{pmatrix} \frac{3}{4}\gamma(2\mathbf{w}_{200}^u + \mathbf{w}_{220}^u + \mathbf{w}_{222}^u) \\ 0 \end{pmatrix} - 2L\mathbf{w}_{200} - \frac{1}{4}\zeta_{00}^{(1)}(\rho, \mathbf{w}_{311}) - \frac{1}{2}\zeta_{00}^{(1)}(\mathbf{w}_{200}, \mathbf{w}_{200}) - \frac{1}{4}\zeta_{00}^{(1)}(\mathbf{w}_{220}, \mathbf{w}_{220}) - \frac{1}{4}\zeta_{00}^{(1)}(\mathbf{w}_{202}, \mathbf{w}_{202})0 - \frac{1}{8}\zeta_{00}^{(1)}(\mathbf{w}_{222}, \mathbf{w}_{222}),$$
$$\mathbf{H}_{11} = \frac{\partial A_1}{\partial T_3}\rho + b^{(3)} A_1 \bar{k}_c^2 \begin{pmatrix} 0 \\ u_0 M + v_0 \end{pmatrix},$$
$$\mathbf{H}_{20}^{(1)} = 2\sigma \mathbf{w}_{220} - \frac{1}{4}\zeta_{20}^{(1)}(\rho, \mathbf{w}_{311}^{(1)}) + 2b^{(2)}\phi_1^2 \begin{pmatrix} 0 \\ M \end{pmatrix} + 4b^{(2)}\phi_1^2 \begin{pmatrix} 0 & 0 \\ v_0 & u_0 \end{pmatrix} \mathbf{w}_{220},$$
$$\mathbf{H}_{20} = \begin{pmatrix} \frac{3}{2}\gamma(\mathbf{w}_{200}^u + \mathbf{w}_{220}^u + \mathbf{w}_{222}^u) \\ 0 \end{pmatrix} - 2L\mathbf{w}_{220} - \frac{1}{4}\zeta_{20}^{(1)}(\rho, \mathbf{w}_{311} + \mathbf{w}_{331}) - \zeta_{20}^{(1)}(\mathbf{w}_{200}, \mathbf{w}_{220}) - \frac{1}{2}\zeta_{20}^{(1)}(\mathbf{w}_{202}, \mathbf{w}_{222}),$$

$$\mathbf{H}_{02}^{(1)} = 2\sigma\mathbf{w}_{202} - \frac{1}{4}\zeta_{02}^{(1)}(\rho, \mathbf{w}_{311}^{(1)}) + 2b^{(2)}\psi_1^2\begin{pmatrix}0\\M\end{pmatrix} + 4b^{(2)}\psi_1^2\begin{pmatrix}0 & 0\\ v_0 & u_0\end{pmatrix}\mathbf{w}_{202},$$

$$\mathbf{H}_{02} = \begin{pmatrix}\frac{3}{2}\gamma(\mathbf{w}_{200}^u + \mathbf{w}_{220}^u + \mathbf{w}_{222}^u)\\ 0\end{pmatrix} - 2L\mathbf{w}_{202} - \frac{1}{4}\zeta_{02}^{(1)}(\rho, \mathbf{w}_{311} + \mathbf{w}_{313}) - \zeta_{02}^{(1)}(\mathbf{w}_{200}, \mathbf{w}_{202}) - \frac{1}{2}\zeta_{02}^{(1)}(\mathbf{w}_{220}, \mathbf{w}_{222}),$$

$$\mathbf{H}_{22}^{(1)} = 2\sigma\mathbf{w}_{222} - \frac{1}{4}\zeta_{22}^{(1)}(\rho, \mathbf{w}_{311}^{(1)}) + 2b^{(2)}\bar{k}_c^2\begin{pmatrix}0\\M\end{pmatrix} + 4b^{(2)}\bar{k}_c^2\begin{pmatrix}0 & 0\\ v_0 & u_0\end{pmatrix}\mathbf{w}_{222},$$

$$\mathbf{H}_{22} = -2L\mathbf{w}_{222} - \frac{1}{4}\zeta_{22}^{(1)}\Big(\rho, \sum_{i,j=1,3}\mathbf{w}_{3ij}\Big) - \zeta_{22}^{(1)}(\mathbf{w}_{200}, \mathbf{w}_{222}) - \zeta_{22}^{(1)}(\mathbf{w}_{202}, \mathbf{w}_{220}),$$

$$\mathbf{H}_{40} = \begin{pmatrix}\frac{3}{2}\gamma(\mathbf{w}_{220}^u + \mathbf{w}_{222}^u)\\ 0\end{pmatrix} - \frac{1}{4}\Big(\zeta_{40}^{(1)}(\rho, \mathbf{w}_{331}) + \zeta_{40}^{(1)}(\mathbf{w}_{220}, \mathbf{w}_{220}) + \frac{1}{2}\zeta_{40}^{(1)} \times (\mathbf{w}_{222}, \mathbf{w}_{222})\Big),$$

$$\mathbf{H}_{04} = \begin{pmatrix}\frac{3}{2}\gamma(\mathbf{w}_{202}^u + +\mathbf{w}_{222}^u)\\ 0\end{pmatrix} - \frac{1}{4}\Big(\zeta_{04}^{(1)}(\rho, \mathbf{w}_{313}) + \zeta_{04}^{(1)}(\mathbf{w}_{202}, \mathbf{w}_{202}) + \frac{1}{2}\zeta_{04}^{(1)} \times (\mathbf{w}_{222}, \mathbf{w}_{222})\Big),$$

$$\mathbf{H}_{42} = \begin{pmatrix}\frac{3}{4}\gamma(\mathbf{w}_{220}^u + \mathbf{w}_{222}^u)\\ 0\end{pmatrix} - \frac{1}{4}\Big(\zeta_{42}^{(1)}(\rho, \mathbf{w}_{331} + \mathbf{w}_{333}) + 2\zeta_{42}^{(1)}(\mathbf{w}_{220}, \mathbf{w}_{222})\Big),$$

$$\mathbf{H}_{24} = \begin{pmatrix}\frac{3}{4}\gamma(\mathbf{w}_{220}^u + \mathbf{w}_{222}^u)\\ 0\end{pmatrix} - \frac{1}{4}\Big(\zeta_{24}^{(1)}(\rho, \mathbf{w}_{313} + \mathbf{w}_{333}) + 2\zeta_{24}^{(1)}(\mathbf{w}_{202}, \mathbf{w}_{222})\Big),$$

$$\mathbf{H}_{44} = \begin{pmatrix}\frac{3}{4}\gamma\mathbf{w}_{222}^u\\ 0\end{pmatrix} - \frac{1}{4}\Big(\zeta_{44}^{(1)}(\rho, \mathbf{w}_{333}) + \frac{1}{2}\zeta_{44}^{(1)}(\mathbf{w}_{222}, \mathbf{w}_{222})\Big).$$

The solvability condition for (28) holds by imposing $T_3 = 0$ and $b^{(3)} = 0$, and the solution is:

$$\mathbf{w}_4 = A_1^2\sum_{i,j=0,2}\mathbf{w}_{4ij}^{(1)}\cos(i\phi_1 x)\cos(j\psi_1 y) + A_1^4\sum_{i,j=0,2,4}\mathbf{w}_{4ij}\cos(i\phi_1 x)\cos(j\psi_1 y), \tag{45}$$

where the vectors $\mathbf{w}_{4ij}$, $i, j = 0, 2, 4$ are the solutions to the following linear systems:

$$L_{ij}^1\mathbf{w}_{4ij}^{(1)} = \mathbf{H}_{ij}^{(1)}, \quad L_{ij}^1\mathbf{w}_{4ij} = \mathbf{H}_{ij}.$$

At $O(\epsilon^5)$, the resulting equation is given in (29), where:

$$\mathbf{P} = \Big(\frac{\partial A_1}{\partial T_4}\rho + \mathbf{P}_{11}^{(1)}A_1 + \mathbf{P}_{11}^{(3)}A_1^3 + \mathbf{P}_{11}^{(5)}A_1^5\Big)\cos(\phi_1 x)\cos(\psi_1 y) + \mathbf{P}^*.$$

In the above equation, $\mathbf{P}^*$ contains terms that automatically satisfy the compatibility condition and:

$$\mathbf{P}_{11}^{(1)} = \sigma\mathbf{w}_{311}^{(1)} + \bar{k}_c^2\begin{pmatrix}0 & 0\\ v_0 & u_0\end{pmatrix}\Big(b^{(2)}\mathbf{w}_{311}^{(1)} + b^{(4)}\rho\Big),$$

$$\mathbf{P}_{11}^{(3)} = \begin{pmatrix}\frac{9}{4}\gamma\mathbf{w}_{311}^u\\ 0\end{pmatrix} - L\mathbf{w}_{311} + 3\sigma\mathbf{w}_{311} - \zeta_{11}^{(1)}\Big(\rho, \mathbf{w}_{400}^{(1)} + \frac{1}{2}\mathbf{w}_{420}^{(1)} + \frac{1}{2}\mathbf{w}_{402}^{(1)} + \frac{1}{4}\mathbf{w}_{422}^{(1)}\Big) - \zeta_{11}^{(1)}\Big(\mathbf{w}_{200}^{(1)} + \frac{1}{2}\mathbf{w}_{220}^{(1)} + \frac{1}{2}\mathbf{w}_{202}^{(1)} + \frac{1}{4}\mathbf{w}_{222}^{(1)}, \mathbf{w}_{311}^{(1)}\Big) + b^{(2)}\bar{k}_c^2\Big(v_{200} + \frac{v_{220}}{2} + \frac{v_{202}}{2} + \frac{v_{222}}{4} + \begin{pmatrix}0\\M\end{pmatrix}\big(u_{200} + \frac{u_{220}}{2} + \frac{u_{202}}{2} + \frac{u_{222}}{4}\big)\Big) + b^{(2)}\bar{k}_c^2\begin{pmatrix}0 & 0\\ v_0 & u_0\end{pmatrix}\mathbf{w}_{311},$$

$$\mathbf{P}_{11}^{(5)} = \begin{pmatrix}\frac{3}{4}\gamma(3\mathbf{w}_{222}^u + \mathbf{w}_{313}^u + 4(\mathbf{w}_{202}^u)^2 + 4\mathbf{w}_{202}^u\mathbf{w}_{222}^u + 2(\mathbf{w}_{222}^u)^2)\\ 0\end{pmatrix} - 3L\mathbf{w}_{311} - \zeta_{11}^{(1)}\Big(\rho, \mathbf{w}_{400}^{(1)} + \frac{1}{2}\mathbf{w}_{420}^{(1)} + \frac{1}{2}\mathbf{w}_{402}^{(1)} + \frac{1}{4}\mathbf{w}_{422}^{(1)}\Big) - \zeta_{11}^{(1)}\Big(\mathbf{w}_{200}^{(1)} + \frac{1}{2}\mathbf{w}_{220}^{(1)} + \frac{1}{2}\mathbf{w}_{202}^{(1)} + \frac{1}{4}\mathbf{w}_{222}^{(1)}, \mathbf{w}_{311}^{(1)}\Big) - \frac{1}{2}\zeta_{11}^{(1)}(\mathbf{w}_{200}, \mathbf{w}_{331}) - \frac{1}{2}\zeta_{11}^{(1)}(\mathbf{w}_{202}, \mathbf{w}_{313}) - \frac{1}{4}\zeta_{11}^{(1)}(\mathbf{w}_{222}, \mathbf{w}_{313} + \mathbf{w}_{331} + \mathbf{w}_{333}).$$

The solvability condition for (29) is

$$\frac{\partial A}{\partial T_4} = \tilde{\sigma} A - \tilde{L} A^3 + \tilde{Q} A^5, \tag{46}$$

where:

$$\tilde{\sigma} = -\frac{\langle \mathbf{P}_{11}^{(1)}, \mathbf{Y} \rangle}{\langle \rho, \mathbf{Y} \rangle}, \qquad \tilde{L} = \frac{\langle \mathbf{P}_{11}^{(3)}, \mathbf{Y} \rangle}{\langle \rho, \mathbf{Y} \rangle}, \qquad \tilde{Q} = -\frac{\langle \mathbf{P}_{11}^{(5)}, \mathbf{Y} \rangle}{\langle \rho, \mathbf{Y} \rangle}. \tag{47}$$

By adding (46) to (33), we can find the Stuart–Landau equation (35), where:

$$\bar{\sigma} = \sigma + \epsilon^2 \tilde{\sigma}, \qquad \bar{L} = L + \epsilon^2 \tilde{L}, \qquad \bar{Q} = \epsilon^2 \tilde{Q}. \tag{48}$$

References

[1] Y. Almirantis, S. Papageorgiou, Cross–diffusion effects on chemical and biological pattern formation, J. Theor. Biol. 151 (1991) 289–311.
[2] P. Becherer, A.N. Morozov, W. van Saarloos, Probing a subcritical instability with an amplitude expansion: an exploration of how far one can get, Physica D 238 (2009) 1827–1840.
[3] R.S. Cantrell, C. Cosner, Spatial Ecology via Reaction–Diffusion Equations, John Wiley, Chichester, UK, 2003.
[4] C. Castellano, S. Fortunato, V. Loreto, Statistical physics of social dynamics, Rev. Mod. Phys. 81 (2009) 592–638.
[5] S.M. Cox, P.C. Matthews, Exponential time differencing for stiff–systems, J. Comput. Phys. 176 (2002) 430–455.
[6] M. Cross, H. Greenside, Pattern Formation and Dynamics in Nonequilibrium Systems, Cambridge University Press, Cambridge, UK, 2009.
[7] M.C. Cross, P.C. Hohenberg, Pattern formation outside of equilibrium, Rev. Mod. Phys. 65 (1993) 851–1112.
[8] G.C. Cruywagen, P.K. Maini, J.D. Murray, Biological pattern formation on two–dimensional spatial domains: a nonlinear bifurcation analysis, SIAM J. Appl. Math. 57 (1997) 1485–1509.
[9] G. Gambino, M.C. Lombardo, M. Sammartino, Pattern formation driven by cross-diffusion in a 2D domain, Nonlinear Anal., Real World Appl. 14 (2013) 1755–1779.
[10] E. Gilad, J. von Hardenberg, A. Provenzale, M. Shachak, E. Meron, A mathematical model of plants as ecosystem engineers, J. Theor. Biol. 244 (2007) 680–691.
[11] E.E. Holmes, M.A. Lewis, J.E. Banks, R.R. Veit, Partial differential equations in ecology: spatial interactions and population dynamics, Ecology 75 (1994) 17–29.
[12] R. Hoyle, Pattern Formation. An Introduction to Methods, Cambridge University Press, Cambridge, UK, 2006.
[13] A.K. Kassam, L.N. Trefethen, Fourth-order time-stepping for stiff PDEs, SIAM J. Sci. Comput. 26 (2005) 1212–1233.
[14] X. Meng, R. Liu, T. Zhang, Adaptive dynamics for a non-autonomous Lotka-Volterra model with size-selective disturbance, Nonlinear Anal., Real World Appl. 16 (2014) 202–213.
[15] J.D. Murray, Mathematical Biology, Springer–Verlag, Berlin, Heidelberg, 2003.
[16] A. Newell, J. Whitehead, Finite band width, finite amplitude convection, J. Fluid Mech. 38 (1969) 279–303.
[17] R.M. Nisbet, W.S.C. Gurney, Modeling Fluctuating Populations, John Wiley, NewYork, 1982.
[18] A. Okubo, Diffusion and Ecological Problems: Mathematical Models, Biomathematics, Springer–Verlag, Berlin, Heidelberg, 1980.
[19] K.M. Owolabi, K.C. Patidar, Numerical simulations for multicomponent ecological models with adaptive methods, Theor. Biol. Med. Model. 13 (2016) 1–25.
[20] Y. Peng, T. Zhang, Stability and Hopf bifurcation analysis of a gene expression model with diffusion and time delay, Abstr. Appl. Anal. 2014 (2014) 1.
[21] Y. Peng, T. Zhang, Turing instability and pattern induced by cross–diffusion in a predator–prey system with Allee effect, Appl. Math. Comput. 275 (2016) 1–12.
[22] M. Perc, A. Szolnoki, Noise–guided evolution within cyclical interactions, New J. Phys. 9 (2007) 267–282.
[23] M. Perc, A. Szolnoki, G. Szabo, Cyclical interactions with alliance specific heterogeneous invasion rates, Phys. Rev. E 75 (2007) 052102.
[24] L.A. Segel, J.L. Jackson, Dissipative structure: an explanation and an ecological example, J. Theor. Biol. 37 (1972) 545–559.
[25] N. Shigesada, K. Kawasaki, E. Teramoto, Spatial segregation of interacting species, J. Theor. Biol. 79 (1979) 83–99.
[26] Y. Song, T. Zhang, Y. Peng, Turing–Hopf bifurcation in the reaction–diffusion equations and its applications, Commun. Nonlinear Sci. Numer. Simul. 33 (2016) 229–258.
[27] A. Szolnoki, M. Mobilia, L.-L. Jiang, B. Szczesny, A.M. Rucklidge, M. Perc, Cyclic dominance in evolutionary games: a review, J. R. Soc. Interface 11 (2014) 20140735–20140755.
[28] A. Szolnoki, M. Perc, Correlation of positive and negative reciprocity fails to confer an evolutionary advantage: phase transitions to elementary strategies, Phys. Rev. X 3 (2013) 041021.
[29] X. Tang, Y. Song, Cross–diffusion induced spatiotemporal patterns in a predator–prey model with herd behavior, Nonlinear Anal., Real World Appl. 24 (2015) 36–49.
[30] L.N. Trefethen, Spectral Methods in MATLAB, SIAM, Philadelphia, PA, USA, 2000.
[31] A.M. Turing, The chemical basis of morphogenesis, Philos. Trans. R. Soc. Lond. B 237 (1952) 37–72.
[32] V.K. Vanag, I.R. Epstein, Cross–diffusion and pattern formation in reaction–diffusion system, Phys. Chem. Chem. Phys. 11 (2009) 897–912.
[33] M. van Hecke, P.C. Hohenberg, W. van Saarloos, Amplitude equations for pattern forming systems, in: M.H. Ernst, H. van Beijeren (Eds.), Fundamental Problems in Statistical Mechanics, VIII, Proceedings of the Eighth International Summer School on Fundamental Problems in Statistical Mechanics, Altenberg, Germany, 28 June–10 July 1993, 1994, pp. 245–278.
[34] D.J. Wollkind, V.S. Manoranjan, L. Zhang, Weakly nonlinear stability analyses of prototype reaction–diffusion model equations, SIAM Rev. 36 (1994) 176–214.
[35] T. Zhang, Y. Xing, H. Zang, M. Han, Spatio–temporal dynamics of a reaction–diffusion system for a predator–prey model with hyperbolic mortality, Nonlinear Dyn. 78 (2014) 265–277.
[36] T. Zhang, H. Zang, Delay–induced Turing instability in reaction–diffusion equations, Phys. Rev. E 90 (2014) 052908.